Integrated Wideband 2-D and 3-D Transitions for Millimeter-Wave RF Front-Ends

Amin Rida, *Student Member, IEEE*, Alexandros Margomenos, *Member, IEEE*, Jae Seung Lee, *Member, IEEE*, Paul Schmalenberg, Symeon Nikolaou, and Manos M. Tentzeris, *Fellow, IEEE*

***Abstract*—This letter reports on broadband 3-D and 2-D transitions on flexible organic liquid crystal polymer (LCP) substrate with return loss below 15 dB for frequencies up to 110 GHz. The presented novel 3-D coplanar waveguide–coplanar waveguide–microstrip (CPW–CPW–MSTRIP) transition features an insertion loss (IL) of 0.45 dB for a 3.3-mm total (longitudinal) length of transition, while the novel 3-D CPW–CPW transition has an IL of 0.25 dB for a 2.8-mm (longitudinal) length of transition. These transitions require strategically placed vias and tapering of the CPW ground planes in order to suppress radiation loss and optimize the performance over a very broad frequency range. This letter also includes a 90° CPW bend that shows a return loss lower than 15 dB up to 100 GHz and an insertion loss of 0.75 dB for a 6.35-mm total length of the transition. All these transitions are simple to realize and are compatible with low-cost substrate fabrication guidelines allowing for the easy integration of ICs in 3-D modules, especially in compact automotive radar applications and beam-steering wideband antenna arrays. An example of the integration of the proposed 3-D transitions with a practical antenna array is presented, and experiments verify the very good performance of the integrated topology up to 100 GHz.**

***Index Terms*—2-D transition, 3-D transition, broadband transition, coplanar waveguide (CPW), integration, microstrip, millimeter-wave.**

I. Introduction

LOW-COST, wideband, and miniaturized RF 3-D and 2-D transitions that are compatible with current state-of-the-art design rules on flexible materials are critical for an effective performance in millimeter-wave frequencies, the use of which is constantly growing to achieve increasingly higher bandwidths or better radar resolutions [1]–[3]. Realizing compact interconnects with low insertion and reflection loss over an ever-increasing frequency range, sometimes reaching above 100 GHz, is paramount for high-sensitivity miniaturized RF applications. Such vertical architectures could potentially eliminate bulky high-loss waveguide transitions that are currently used in many broadband millimeter-wave systems, especially in the field of automotive radars [4].

In addition to the 3-D transitions, the planar or 2-D transitions of microstrip and coplanar waveguide (CPW) lines become a critical part of RF modules with large antenna arrays. This is due to the far more stringent spatial requirements on the spacing and separation distances among the subarray antenna elements (typically $\lambda/2$) in comparison to the interconnection spacing among the feeding lines to multichannel T/R modules or ICs ($< \lambda/2$).

The purpose of this letter is to describe a method for the development of easy-to-fabricate low-cost 3-D and 2-D transitions on the flexible organic liquid crystal polymer (LCP) [5] for use in millimeter-wave (up to 100 GHz) front-end applications such as broadband high-speed wireless LAN [1], automotive radar, and imaging systems. LCP has recently gained much consideration as a potential high-performance microwave medium with excellent "dual" (substrate and packaging) functionality due to its very good electrical, mechanical, and hermeticity properties, not to mention its attractive high-frequency properties for developing millimeter-wave circuitry [5]. In addition, LCP can be easily laminated and micromachined to form 3-D multilayer modules. Due to its near-hermetic characteristic, LCP can be easily used for the integration of embedded bare ICs without the use of additional packaging material—something that allows for the module miniaturization, but also necessitates the development of broadband low-loss 3-D CPW-to-CPW and CPW-to-microstrip (MSTRIP) interconnects. For the purpose of this work, the dielectric characterization of the utilized LCP material was performed using a free-space method [6], and the dielectric constant ($\varepsilon_{\rm r}$) was measured to be around 3.0 for the frequencies of interest.

II. Wideband 3-D Transitions

A recently reported 3-D micromachined transition on Si features good performance up to 50 GHz [7], but it is very costly due to the tedious formation of cavities. In [8], another broadband vertical transition has been realized, however with supported measurement results up to 60 GHz and with a four-layer cross section. In [9], an ultrawideband microstrip-to-CPW transition has been reported with a 0.7-dB transition up to 40 GHz. Other reported efforts, such as [10], utilize waveguide-to-microstrip line transitions from one layer to another. However, they are bulky and limited in bandwidth, and they require the use of waveguide-based topologies. In this letter, two simple wideband

Manuscript received September 09, 2010; revised November 03, 2010; accepted November 04, 2010. Date of publication November 11, 2010; date of current version November 29, 2010. This work was supported by the Interconnect Focus Center, Semiconductor Research Corporation (IFC-SRC), Atlanta, GA.

A. Rida, S. Nikolau, and M. M. Tentzeris are with the Electrical Engineering Department, Georgia Institute of Technology, Atlanta, GA 30332 USA (e-mail: arida@gatech.edu; simos.nikolaou@gmail.com; etentze@gatech.edu).

A. Margomenos was with Toyota Research Institute North America, Ann Arbor, MI 48105 USA. He is now with HRL Laboratories, LLC, Malibu, CA 90265 USA (e-mail: admargomenos@hrl.com).

J. S. Lee and P. Schmalenberg are with Toyota Research Institute North America, Ann Arbor, MI 48105 USA (e-mail: jae.lee@tema.toyota.com; paul.schmalenberg@tema.toyota.com).

Color versions of one or more of the figures in this letter are available online at http://ieeexplore.ieee.org.

Digital Object Identifier 10.1109/LAWP.2010.2091714

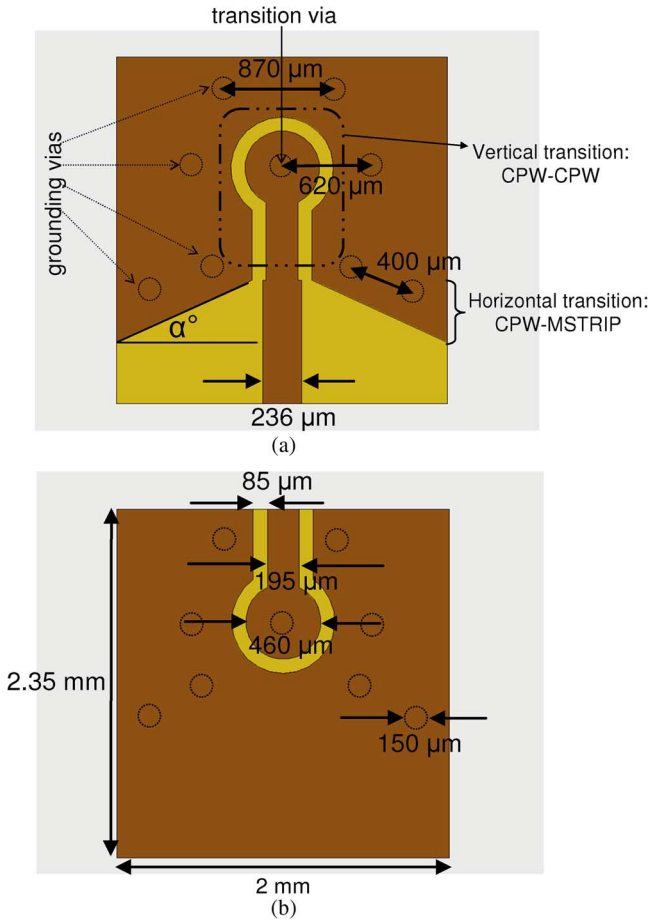

Fig. 1. Schematic for wideband vertical CPW–CPW–MSTRIP transition. (a) Top view. (b) Bottom view.

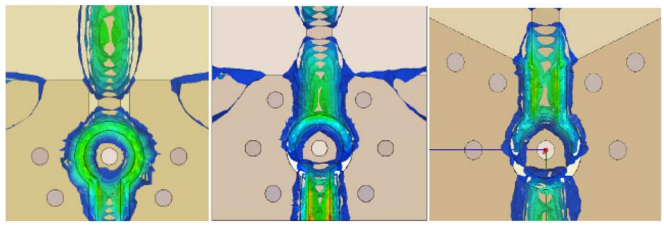

Fig. 2. E-field distribution at 76.5 GHz for the design stages in the CPW–CPW–MSTRIP transition.

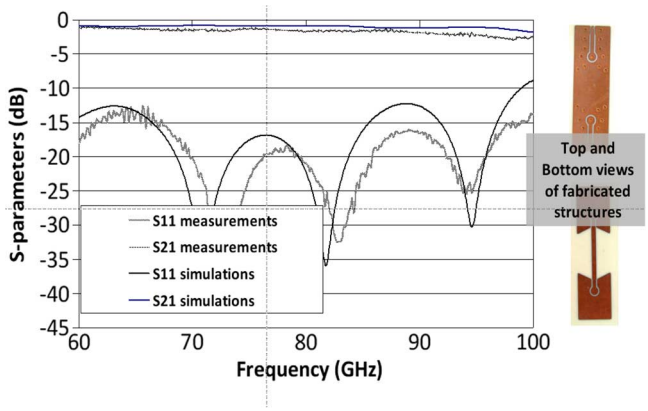

Fig. 3. S-parameters and photographs of the fabricated structure for CPW–CPW–MSTRIP transition.

3-D transitions, one for CPW–CPW–MSTRIP line and another for CPW–CPW–CPW line, will be presented on LCP and up to 100 GHz utilizing two layers of metallization only. Both of these consist of a vertical and a horizontal transition. All dimensions on the designed structures are based on existing commercially available design rules and the use of mechanical drilling for via formation.

A. CPW–CPW–MSTRIP Transition

The proposed design achieves a very good wideband RF performance by utilizing a tapered ground plane and by placing grounding vias in appropriate locations in order to suppress parasitic modes and eliminate radiation losses due to open-end effects. The via pads and gaps are optimized so as to match the series inductance of the via transition and maintain a 50-Ω characteristic impedance throughout the transition, allowing for a very broadband response up to 100 GHz.

Furthermore, the design consists of one via-based vertical transition used to connect the CPW signal (center) transmission lines printed on both sides of a single LCP layer ($\sim$ 100 μm thick), as well as grounding vias connecting the top and bottom ground layers. Fig. 1 shows in detail the design schematic with the specific via placements. The effect of the strategically chosen placement of the vias is demonstrated in the field plot shown in Fig. 2, which signifies the importance of having the ground tapered with a specific angle in order to suppress all E-field edge radiation effects.

The bottom layer [Fig. 1(b)] starts as a CPW launch with characteristic impedance Z_0 of 50 Ω, realized appropriately choosing the signal line width and the gap between the signal line and the ground. The CPW slot width ($\sim$85 μm) is responsible for maintaining a desired CPW mode for the wide frequency band up to 100 GHz throughout the CPW section of the transmission line (top and bottom), so it is kept at a constant value around the via pad, resulting in minimum field reflections and very good impedance matching.

The transition via lies within a wide circular disk shape to accommodate for the via pad, which has an extra 300 μm larger radius compared to the via one (75 μm), which is specified by the fabrication requirements for metallization purposes. A 75-μm via diameter was chosen. This dimension is the smallest diameter that could be mechanically drilled and metallized, thus determining the smallest via size with a satisfactory RF performance. The CPW ground planes on the top layer have been tapered at an angle α of $\sim 27^\circ$. The tapering of the CPW ground has been utilized in previous work such as [9] for an optimized transition between the CPW and the microstrip, and the value α was chosen based on simulation optimizations. Fig. 3 shows the results for the simulated and measured S-parameters, exhibiting good agreement over a very broadband response.

The simulations were performed using Ansys HFSS. The insertion loss (IL) of the whole structure with back- to-back transition as shown in Fig. 3 and for a total length of 6.6 mm (length of the back-to-back module starting with CPW line on one side of the substrate, transitioning to CPW line on the other side of the substrate, then in turn transitioning to microstrip line) is 0.9 dB

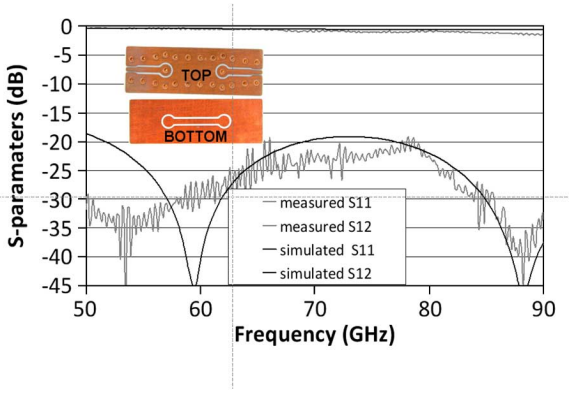

Fig. 4. S-parameters and photograph of the fabricated structure for 3-D CPW–CPW transition.

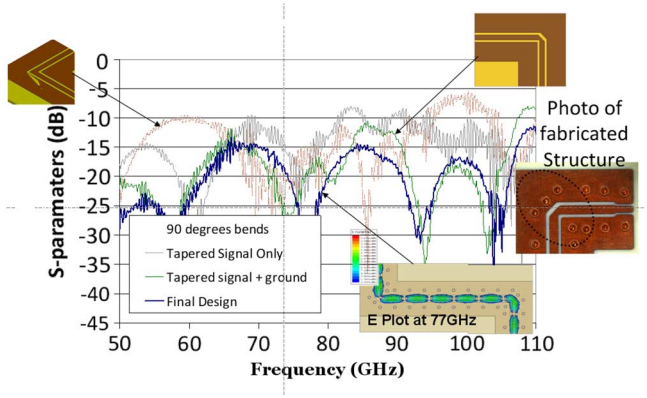

Fig. 5. S_{11} for the step-by-step design process for the CPW bends.

after deembedding the input launch lines corresponding to an IL of 0.45 dB per transition (of length 3.3 mm) at 77 GHz and 1.175 dB at 100 GHz.

B. 3-D CPW–CPW Transition

The same design approach was followed for designing a wideband 3-D CPW–CPW. This design features only CPW transmission lines (Fig. 4), thus it contains one less transition in comparison to Section II-A. However, it was chosen as the showcasing structure for the critical importance of the optimal via spacing for a broadband satisfactory ground equalization between the top and bottom ground layers for the CPW lines. The S-parameter results are presented in Fig. 4, exhibiting a return loss below 20 dB for the 50–90-GHz frequency range. The insertion loss is 0.5 dB at 77 GHz for the back-to-back transition of total length 5.6 mm, or equivalent to 0.25 dB IL for a single transition of total length 2.8 mm. For this design, the major focus was the selection of the optimum number of and spacing between the vias in the CPW section. Maintaining a 600-μm $(\sim \lambda_g/4)$ via–via spacing was necessary in order to suppress the parasitic radiation due to the parallel-plate CPW mode and achieve good performance while keeping the transition and the resulting front-end real estate at a minimum.

III. Wideband 2-D Transitions Up to 110 GHz

Previous work in CPW and CPW-G bends have considered the use of air bridges [11], which add cost and mechanical limitations to the circuit fabrication. In [12], slow wave compensation, requiring very stringent fabrication tolerances, was used to optimize the CPW bend up to 50 GHz.

In this letter, a design approach that allows wideband, high-performance 90° bends on grounded coplanar waveguide (CPWG) is presented for operability up to 110 GHz. Both signal and ground planes are chamfered, and the CPWG line uses periodic vias placed at 750-μm separation with a radius of 75 μm for reasons similar to those stated before in Sections II-A and II-B (for optimal RF performance; suppression of the parallel-plate and slot-line modes for the minimum number of vias). The location of the additional vias at the bend is very critical for the performance optimization of the bend, as shown in Fig. 5, which demonstrates the step-by-step optimization procedure of the S_{11}-parameters (measurements)

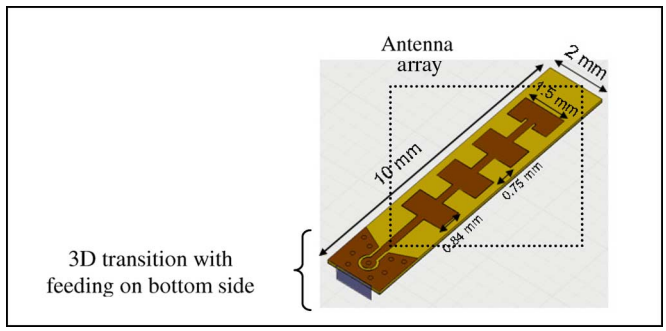

Fig. 6. Schematic of the integration of 3-D CPW–MSTRIP transition with four-element patch antenna array.

starting with a 90° CPWG bend, then chamfering or tapering the signal line only, followed by the tapering of both signal and ground lines, and eventually the final design that includes the placement of additional strategically positioned vias around the bend. Upon chamfering the bend, one can observe the improvement in the performance only up to 75 GHz, while the vias optimize the performance above 75 GHz. The final design features a very good performance at frequencies up to 110 GHz with a return loss lower than 15 dB. The insertion loss of the structure of total length 12.7 mm consisting of two CPW (back-to-back) bends is 1.5 dB at 77 GHz, equivalent to 0.12 dB/mm of the CPW bend structure. These results are reported for the first time for frequencies up to 110 GHz and for simple-to-fabricate 2-D transition topologies.

IV. Integration of 3-D Transitions With Antenna Array

The easy integrability of the proposed interconnects can be demonstrated in Fig. 6 showing the integrated topology of the CPW–CPW–MSTRIP 3-D transition with a four-element microstrip antenna array, designed to resonate at the automotive millimeter-wave radar frequency of 77 GHz.

The S_{11} parameters are shown in Fig. 7 to exhibit good response with a minor shift in resonance frequency due to etching effects and/or the process tolerances in manufacturer's dielectric properties, especially that of ε_r. The simulated radiation efficiency (at 77 GHz) was found to be 75% and a total gain of 10 dBi. With an overall good agreement, this verifies the proof of concept of the easy and effective integration of the proposed

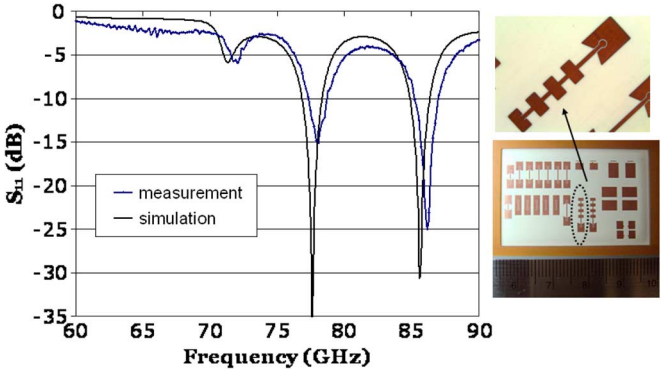

Fig. 7. S_{11} results for the integrated 3-D CPW–MSTRIP transition with the four-element patch antenna array.

3-D transitions with practical antenna arrays to be used in large array systems for millimeter-wave applications such as automotive radars.

This integrated configuration would be especially useful as a radiation reduction mechanism between the feed network and/or the mounted IC packages with the antenna array. This is achieved by suppressing any undesired radiation that could be due to sharp edges and/or significant electrical length of the feeding lines as well as mismatches between the feeding lines and the IC, which could be detrimental for the radiation performance of the antenna array.

V. Conclusion

This letter presented two novel broadband 3-D vertical transitions and one 2-D transition or CPW bend on flexible organic liquid crystal polymer substrate that demonstrate an excellent performance up to 100 GHz. The transitions are implemented on a single LCP layer, are easily realizable, and are compatible with low-cost substrate fabrication guidelines. This makes them very appealing for cost-sensitive applications. The presented design is a critical component of highly integrated 3-D RF front-ends that demonstrates the capabilities of LCP to form high-performance, broadband, low-cost, system-in-package conformal broadband architectures up to 100 GHz. In addition, there is a great advantage to isolate any radiation from a feeding network or interconnections from an IC to the millimeter-wave antenna arrays, and so this method of integrating a 3-D transition would come into play as a radiation reduction mechanism.

Acknowledgment

The authors would like to acknowledge the Interconnect Focus Center and the Semiconductor Research Center for their support. The authors would also like to acknowledge the facilities that carried out the fabrication of the structures featured: Metro Circuits (Rochester, NY) and Hughes Circuits (San Marcos, CA).

References

[1] S. Q. Xiao, *Millimeter Wave Technology in Wireless PAN, LAN, and MAN*. Boca Raton, FL: CRC Press, 2008.

[2] J. Schoebel, T. Buck, M. Reimann, M. Ulm, M. Schneider, A. Jourdain, G. Carchon, and H. A. C. Tilmans, "Design considerations and technology assessment of phased-array antenna systems with RF MEMS for automotive radar application," *IEEE Trans. Microw. Theory Tech.*, vol. 53, no. 6, pp. 1968–1975, Jun. 2005.

[3] S. Beer, G. Adamiuk, and T. Zwick, "Novel antenna concept for compact millimeter-wave automotive radar sensors," *IEEE Antennas Wireless Propag. Lett.*, vol. 8, pp. 771–774, 2009.

[4] M. Steinhauer, H.-O. Ruov, H. Irion, and W. Menzel, "Millimeter-wave radar sensor based on a transceiver array for automotive applications," *IEEE Trans. Microw. Theory Tech.*, vol. 56, no. 2, pp. 261–269, Feb. 2008.

[5] D. C. Thompson, O. Tantot, H. Jallageas, G. E. Ponchak, M. M. Tentzeris, and J. Papapolymerou, "Characterization of liquid crystal polymer (LCP) material and transmission lines on LCP substrates from 30–110 GHz," *IEEE Trans. Microw. Theory Tech.*, vol. 52, no. 4, pp. 1343–1352, Apr. 2004.

[6] Agilent Technologies, "Agilent 8571E materials measurement software. Technical overview," Santa Clara, CA, May 2010 [Online]. Available: http://cp.literature.agilent.com/litweb/pdf/5988-9472EN.pdf

[7] A. Margomenos, Y. Lee, and L. P. B. Katehi, "Wideband Si micromachined transitions for RF wafer-scale packages," in *Proc. IEEE SiRF*, Long Beach, CA, Jan. 2007, pp. 183–186.

[8] A. Stark and A. F. Jacob, "A broadband vertical transition for millimeter-wave applications," in *Eur. Microw. Conf. 2008 Dig.*, Amsterdam, The Netherlands, Oct. 2008, pp. 476–479.

[9] Y. G. Kim, K. W. Kim, and Y. K. Cho, "An ultra-wideband microstrip-to-CPW transition," in *Proc. IEEE MTT-S Int. Microw. Symp.*, 2008, pp. 1079–1082.

[10] W. Mayer, M. Meilchen, W. Grabherr, P. Nuchter, and R. Guhl, "Eight-channel 77-GHz front-end module with high performance synthesized signal generator for FMCW sensor applications," *IEEE Trans. Microw. Theory Tech.*, vol. 52, no. 3, pp. 993–1000, Mar. 2004.

[11] N. H. L. Koster, S. Koblowski, R. Bertenburg, S. S. H. S. Heinen, and I. A. W. I. Wolff, "Investigations on air bridges used for MMICs in CPW technique," in *Proc. 19th Eur. Microw. Conf.*, Sep. 1989, pp. 666–671.

[12] H. Kim and R. F. Drayton, "Wire-bond free technique for right-angle coplanar waveguide bend structures," *IEEE Trans. Microw. Theory Tech.*, vol. 57, no. 2, pp. 442–448, Jan. 2009.